Original article

Employing a PLGA-TPGS based nanoparticle to improve the ocular delivery of Acyclovir

Musaed Alkholief [a], Hammam Albasit [a], Adel Alhowyan [a], Sultan Alshehri [b], Mohammad Raish [b], Mohd Abul Kalam [a], Aws Alshamsan [a,*]

[a] Nanobiotechnology Unit, Department of Pharmaceutics, College of Pharmacy, King Saud University, Riyadh, Saudi Arabia
[b] Department of Pharmaceutics, College of Pharmacy, King Saud University, P.O. Box: 2457, Riyadh 11451, Saudi Arabia

ARTICLE INFO

ABSTRACT

Delivering drugs via the ocular route has always been a challenge for poorly soluble drugs. The various anatomical and physiological barriers in the eye cavity hinder the residence of drugs within the corneal and precorneal regions. In this study, the nanosystem that could sufficiently deliver the poorly soluble Acyclovir topically via ocular route. Our nanosystem is composed of the biocompatible PLGA polymer stabilized with TPGS which possess a high emulsifying capacity and is also known as P-gp inhibitor. The optimized nanoparticles were prepared with 0.3% TPGS and had particle-size of 262.3 nm, zeta-potential of +15.14 mV. The physicochemical-characterization, *ex vivo* transcorneal permeation, ocular-irritation and Acyclovir ocular-availability, following topical ocular application of PLGA-NPs in rabbit eyes, were performed. The tested parameters and irritation by Draize's test suggested the suitability and safety of PLGA-NPs for ocular use. An ultrahigh performance liquid chromatographic method was developed, validated, and applied to quantify Acyclovir in aqueous humor which was shown to be significantly higher ($p < 0.05$) using the developed nanoparticles as compared to Acyclovir-aqueous suspension following their single topical ocular administration. Noticeable 2.78-, 1.71- and 2.2-times increased values of AUC_{0-24h}, $t_{1/2}$ (h) and MRT_{0-24h} were found, respectively, with the PLGA-TPGS-NPs as compared to ACY-AqS. These results demonstrate the superiority of delivering Acyclovir using a nanosystem compared to conventional methods.

© 2018 The Authors. Production and hosting by Elsevier B.V. on behalf of King Saud University. This is an open access article under the CC BY-NC-ND license (http://creativecommons.org/licenses/by-nc-nd/4.0/).

1. Introduction

Despite its limitations, topical application to the eye remains the preferred route of ocular drug administration. The process of delivering drugs to the eye via topical administration is hindered by extremely-defensive anatomical and physiological barriers, resulting in poor ocular bioavailability (Cholkar et al., 2013; Fangueiro et al., 2014). These barriers include the efficient and prompt nasolacrimal drainage, noncorneal absorption,

P-glycoprotein (P-gp) efflux mechanism, and impermeability towards hydrophilic/hydrophobic drugs (Cholkar et al., 2013). Consequently, only 5% of the administered-drop dose penetrates the cornea to the anterior ocular tissues (Fabiano et al., 2015; Seyfoddin et al., 2010). Therefore, it is thought that prolonging precorneal drug retention and enhancing its permeation would remarkably improve bioavailability and efficacy of drugs. One possible strategy is by employing nanoparticles (NPs)-based delivery in order to overcome some inadequacies of traditional eye formulations (Akhter et al., 2013; Warsi et al., 2014).

In this study, we utilized poly-(D,L-lactic-*co*-glycolic acid) (PLGA), which is a biodegradable and biocompatible anionic polymer with hydrophobic nature that has been approved long ago by FDA for human use (Akhter et al., 2013; Chen et al., 2011; Danhier et al., 2012). Although previous studies have shown that PLGA-NPs could bypass P-gp efflux (Nagarwal et al., 2009; Salama et al., 2015; Warsi et al., 2014), we argue that the addition of another P-gp-antagonizing moiety would enhance PLGA-NPs permeation through the cornea. Moreover, the biodegradation of PLGA takes place through a three-phase mechanism. First, little decrease

Production and hosting by Elsevier

in the molecular weight without considerable weight loss of PLGA occurs. Second, a significant and rapid loss of molecular mass occurs, where the formation of soluble monomers and oligomers take place. In the third phase, soluble oligomers get converted into soluble monomers and resulting in the complete biodegradation of PLGA (Jain, 2000). Since stabilizers are frequently used in PLGA-NPs preparation processes, we applied D-α-Tocopherol polyethylene glycol 1000 succinate (vitamin E-TPGS) as a stabilizer (Zhang et al., 2008), which is also known to inhibit corneal P-gp (Chen et al., 2011). Being a P-gp inhibitor, TPGS was thought to improve transcellular or transcorneal permeability of drugs, hence could improve drug absorption and reduce P-glycoprotein-mediated multidrug resistance (Dintaman and Silverman, 1999; Ma et al., 2010). Because of its amphiphilic nature, TPGS provides over 70-fold higher emulsification and stabilizing efficiency as compared to polyvinyl alcohol (PVA) and polyvinylpyrrolidone (PVP) (Warsi et al., 2014). As a result, TPGS-emulsified NPs have shown high drug encapsulation, cellular uptake, and therapeutic efficacy (Ma et al., 2010). With such a delivery system, transcorneal permeation of drugs with poor ocular bioavailability can be remarkably enhanced. Given all the potential advantages of using TPGS-emulsified PLGA-NPs, we employed these NPs for ocular delivery of acyclovir (ACY), which is a synthetic acyclic analogue of 2, 9-deoxyguanosine that has been approved as a potent and selective inhibitor of the replication of *Herpes simplex* type-1, type-2, and *Varicella zoster* viruses. ACY acts by inhibiting viral DNA replication following its conversion to ACY monophosphate, and then ACY triphosphate by the enzyme thymidine kinase (Law et al., 2000; Naderkhani et al., 2014; Stulzer et al., 2008). Due to its poor ocular bioavailability, present study aims at increasing ocular bioavailability of ACY through PLGA-NPs stabilized with vitamin E-TPGS.

2. Materials and methods

2.1. Materials

ACY, PLGA (50:50, Mw 30,000–60,000), polyvinylpyrrolidone (average Mw 40,000) and vitamin E-TPGS were purchased from Sigma-Aldrich (St. Louis, MO, USA). Mannitol was purchased from Qualikems Fine Chem Pvt. Ltd, Vadodara, India. Ammonium acetate was purchased from Fluka Chemika, Switzerland. Acetic acid glacial was purchased from BDH Limited (Poole, England). Acetonitrile HiPerSolv CHROMANORM for HPLC grade was purchased from BDH, PROLABO, LEUVEN, EC. Milli-Q® (Millipore, France) purified water, analytical grade chemicals and HPLC grade solvents were used in this study.

2.2. Preparation and characterization of ACY-loaded PLGA nanoparticles

2.2.1. Nanoparticles preparation

ACY-loaded PLGA-NPs (ACY-PLGA-NPs) were prepared by nano-precipitation technique (Alshamsan, 2014). Briefly, 100 mg PLGA

was dissolved in 1 mL acetone. A specific amount of ACY (5, 10, or 15 mg) was dissolved into the PLGA solution and then added dropwise to 10 mL of continuously stirring varying concentrations of vitamin E-TPGS solution (0.1, 0.3 or 0.6% w/v). Acetone was allowed to evaporate by continuous magnetic stirring for 4 h. ACY-PLGA-NPs were then recovered from the nano-dispersion by centrifugation at 15,000 rpm for 35 min at 4 °C using (PRISM-R, Labnet International Inc. Edison, NJ, USA) ultracentrifuge. Then, precipitated PLGA-NPs were suspended in mannitol solution (2.5, 5 or 7.5% w/v) and lyophilized for 72 h in FreeZone 4.5 Freeze Dry System (Labconco Corporation, Kansas City, MO, USA). Another group of nanoparticles were prepared following similar technique but using PVP solution (0.5, 1 and 1.5% w/v) instead of vitamin E-TPGS as mentioned in Table 1.

2.2.2. Physicochemical characterization of ACY-PLGA-NPs

Particle size, polydispersity (PDI), and zeta potentials of ACY-PLGA-NPs were determined by Zetasizer Nano-Series (Nano-ZS, Malvern Instruments Limited, Worcestershire, UK). ACY entrapment was indirectly determined by measuring the concentration of the unentrapped drug. Briefly, 5 mg of ACY-PLGA-NPs was placed in Eppendorf tubes and dissolved with 250 μL acetone. The acetone was evaporated under a nitrogen stream and the precipitant was re-suspended in 500 μL of 0.1 M sodium hydroxide solution to dissolve ACY only while precipitating PLGA. Then, ACY concentration in the supernatant was determined by the ultra-performance liquid chromatography (UPLC) with UV-detection at 254 nm wavelength by modifying a previously-reported HPLC method for ACY analysis (Grenha et al., 2007; Silva et al., 2013). The encapsulation efficiency (%EE) and drug loading (%DL) were calculated using Eqs. (1) and (2), respectively.

$$\% \ EE = \left(\frac{Total \ drug \ amount \ (\mu g) - Unentrapped \ drug \ amount \ (\mu g)}{Total \ drug \ amount \ (\mu g)} \right) \times 100 \tag{1}$$

$$\% \ DL = \left(\frac{Total \ drug \ amount \ (\mu g) - Unentrapped \ drug \ amount \ (\mu g)}{Total \ solids \ amount \ (\mu g)} \right) \times 100 \tag{2}$$

Surface morphology of ACY-PLGA-NPs was observed by scanning electron microscope (SEM) (Zeiss EVO LS10; Cambridge, United Kingdom) using gold sputter technique. The dried ACY-PLGA-NPs were coated with gold in Q150R Sputter unit from Quorum Technologies Ltd. (East Sussex, UK) in argon atmosphere at 20 mA for 60 s. The accelerating voltage 10–20 kV and magnification zone for SEM images were kept at 10–15 KX. Moreover, nanosuspension clarity was evaluated by visual examination under light against a white and black background. Also, pH was measured by a calibrated pH meter (Mettler Toledo MP-220, Switzerland) and the refractive index was determined by Abbe refractometer

Table 1
Physical characteristics of ACY loaded PLGA-NPs.

PLGA-NPs	Particle size (nm) ± SD	Polydispersity ± SD	Zeta-potential (mV) ± SD	% Encapsulation ± SD	% Drug loading ± SD
With polyvinylpyrrolidone (PVP, w/v)					
0.5%, (F1)	785.35 ± 35.91	0.484 ± 0.008	−14.51 ± 7.01	58.42 ± 3.58	5.92 ± 1.06
1.0%, (F2)	**174.46 ± 15.25**	**0.297 ± 0.015**	**−15.82 ± 3.69**	**60.25 ± 4.92**	**6.75 ± 1.32**
1.5%, (F3)	295.51 ± 17.38	0.222 ± 0.012	−6.04 ± 3.77	63.34 ± 3.85	7.26 ± 1.41
With D-α-tocopheryl polyethylene glycol 1000 succinate (TPGS, w/v)					
0.1%, (F4)	293.61 ± 13.78	0.257 ± 0.013	15.28 ± 2.05	32.72 ± 2.98	7.67 ± 1.23
0.3%, (F5)	**262.38 ± 11.85**	**0.255 ± 0.011**	**15.14 ± 2.81**	**74.12 ± 6.19**	**8.65 ± 1.09**
0.6%, (F6)	716.15 ± 39.23	0.416 ± 0.023	11.67 ± 1.62	80.15 ± 7.85	5.15 ± 1.38

The values in bold indicate the selected formulation and its parameters.

(model DR-A1, ATAGO, USA. Inc.). The surface tension was measured with a digital tensiometer KlOST (Kruss, Germany). Viscosity was determined by cone and plate viscometer (Physica Rheolab, Austria) using MK-22 spindle. All experiments were done at 25 °C.

2.2.3. In-vitro release in simulated tear fluid

Lyophilized ACY-PLGA-NPs were suspended in isotonic mannitol solution (5%, w/v) and then diluted by simulated tear fluid (STF) containing 0.68 g NaCl, 0.22 g NaHCO$_3$, 0.008 g CaCl$_2$·2H$_2$O and 0.14 g KCl in 100 mL Milli-Q® water, where the final concentration of acyclovir was 0.28% (w/v). In Eppendorf tubes, 1-mL aliquots of the dispersion were placed on floating pads, and kept in shaking water bath (100 rpm) at 37 °C. At designated time points, a set of triplicate samples was removed and centrifuged at 13,500 rpm for 30 min at 10 °C. Afterwards, supernatants were collected and the concentration of released ACY was analyzed by UPLC at 254 nm detection wavelength (Law et al., 2000). Next, ACY release data were subjected to goodness of fit test by linear regression analysis method applying different kinetic equations such as zero-order, first-order, Higuchi's square-root plot, Korsmeyer-Peppas and Hixson-Crowell cube-root plot. The model equation giving a correlation coefficient (R^2) value close to unity will be considered as the order of release.

2.2.4. Stability of ACY-PLGA-NPs

In 10-mL glass scintillation vials, samples of ACY-PLGA-NPs were stored for 3 months at 25 ± 0.5 °C away from direct sunlight exposure. The physical stability of ACY-PLGA-NPs was assessed by following the reported methods (De and Robinson, 2004; Kalam, 2016a). About 5 mg of ACY-PLGA-NPs were dispersed in 5 mL STF. Then, changes in particle-size, zeta-potential, polydispersity, drug entrapment, and cumulative release of ACY were examined at 1 week, 1 month and 3 months during storage period. To observe the temperature effect on magnitude of aggregation during storage time, ACY-PLGA-NPs were incubated at 4 °C, 25 °C, 37 °C, and 50 °C for 10 days and then samples were observed by SEM.

2.3. Transcorneal permeation

Transcorneal permeation and calculation of permeation parameters were performed following a previously reported method (Attama et al., 2008) employing double-jacketed automated transdermal diffusion cell (sampling system-SFDC 6, LOGAN, New Jersy, USA). In brief, freshly-excised rabbit cornea was fixed between donor and receptor compartments of diffusion cells, where corneal epithelial surface faced towards donor compartment. The receptor compartment was filled with STF (pH7.4). The temperature of water flowing in outer jacket of diffusion cell was 37 ± 1 °C under 95%: 5% (air: CO$_2$) aeration. The fluid in receptor compartment was on magnetic stirring (500 rpm) for removal of air bubbles throughout the study. Then, 600 μL of free ACY solution (ACY-AqS) and ACY-PLGA-NPs suspension containing 0.28% (w/v) was applied to corneal epithelial surface i.e. donor compartment. From the receptor compartment, samples (1 mL) were withdrawn at different time points up to 6 h and equal volume fresh STF was transferred in to the receptor compartment to maintain the sink condition, then permeated amount of ACY was analyzed by UPLC. The amounts of drug permeated (μg·cm^{-2}) through the cornea were plotted against time (h) and slope of the linear portion of the plot was estimated for the determination of permeation parameters. The steady-state flux (J) across the cornea was estimated from linear ascents of permeation plot by the following equation (Eq. (3)),

$$J \left(\mu g \cdot cm^{-2} \cdot s^{-1} \right) = dQ/dt \tag{3}$$

where 'Q' is the amount of drug crossed through the cornea or dQ/dt is linear portion of the slope and 't' is the time of exposure. The permeation coefficient (P) was estimated by the following equation (Eq. (4)).

$$P \left(cm \cdot s^{-1} \right) = J/C_0 \tag{4}$$

where C_0 is the initial drug concentration (μg·mL^{-1}) in the donor compartment.

2.4. In vivo study

2.4.1. Animals

Male albino rabbits weighing 3–4 kg were obtained from the Experimental Animal Care Center, College of Pharmacy, King Saud University, Riyadh, Saudi Arabia. Animals were maintained according to the Guide for the Care and Use of Laboratory Animals approved by the center, and were given pellet diet with water *ad libitum* and fasted overnight before experiments. All animal studies were approved by the Experimental Animal Care Center Review Board (C.P.R.3526)

2.4.2. Ocular Pharmacokinetics (PK)

ACY concentration in aqueous humor in rabbits eyes were assayed in order to check ocular bioavailability following ACY-PLGA-NPs administration as compared with 0.28% (w/v) ACY-AqS. For this reason, 6 rabbits were divided in two groups: group-A for ACY-PLGA-NPs and group-B for ACY-AqS. To each respective group, 50 μL containing 140 μg of ACY were instilled into cul-de-sac of left eyes either in particulate or soluble drug formulation (Kalam, 2016a). After 30 min, animals were anesthetized with an intravenous injection of ketamine.HCl (15 mg·kg^{-1}) and xylazine (3 mg·kg^{-1}). Then, 50 μL of aqueous humor was withdrawn using a 27-gauge needle fitted in insulin syringe through a partial thickness limbal relaxing incision at different time points (Shen et al., 2014). The collected samples were analyzed by UPLC.

2.4.3. Ocular irritation study

Draize's test protocol was followed for ocular irritation study in rabbit eyes (Draize et al., 1944). Briefly, 50 μL of PLGA-TPGS-NPs suspension was put in to the lower conjunctival sac of left eyes of four rabbits and the right eyes of the animals were treated with normal saline as control. The upper and lower eyelids were smoothly held together for few seconds to avoid the loss of instilled dose due to instant tear dilution effect. The sample was administered three times a day for 10 days, and rabbits' eyes were visually observed during the study period. The ocular irritation levels were estimated as per the scoring guidelines, based on the animal discomfort and uneasiness, signs and symptoms in conjunctiva, cornea, and iris according to the reported studies (Diebold et al., 2007; Kalam, 2016b).

2.5. Statistical analysis

All PK parameters were resolved by non-compartmental PK-analysis method (PK-Solver, Nanjing, China in MS-Excel-2013) (Zhang et al., 2010). ACY concentration in aqueous humor was estimated from the relative recovery of ACY in the aspirated aqueous humor samples. The results were articulated as mean ± SD and analyzed for statistical significance ($p < 0.05$) by Paired t-test (GraphPad Software Inc. San Diego, USA).

3. Results and discussion

3.1. Preparation of and characterization of ACY-PLGA-NPs

Optimally, when ocular delivery is intended, small-sized monodispersed nanosystems are preferred over larger polydispersed counterparts as the latter may lead to ocular irritation and discomfort (Zimmer and Kreuter, 1995). The nanosystem (ACY-PLGA-NPs) was prepared by nanoprecipitation method by using PLGA (100 mg) with either PVP or vitamin E-TPGS as stabilizers. The %EE and %DL of ACY-PLGA-NPs prepared with 1%, w/v of PVP (F2) were 60.25% and 6.75%, respectively, while they were 74.12% and 8.65%, respectively, when vitamin E-TPGS (0.3%) was used (F5) (Table 1). Moreover, the average particle size was in the range of 174 nm to 785 nm when PVP was used, whereas it was in the range of 262 nm to 716 nm when vitamin-E TPGS was used. PLGA-PVP-NPs having average size of 785 nm were obtained by adding 1 mL of acetone to 100 mg PLGA, and by using 0.5%, w/v PVP in the aqueous emulsifying phase, where NPs with average size of 174 nm were obtained by using 1.0%, w/v PVP in the same organic phase conditions with almost comparable encapsulation efficiency values but varying loading of ACY (Table 1). Similarly, PLGA-TPGS-NPs with larger sizes (716 nm) were obtained at 0.6%, w/v TPGS concentration yielding the highest encapsulation efficiency value but the lowest loading of the drug. NPs with an average sizes (262 nm), which is an acceptable range for ocular use, was obtained at 0.3% TPGS concentration and yielded a sufficiently higher encapsulation efficiency value and loading of ACY, which was an agreement with the previously reported methods (Collnot et al., 2010; McCall and Sirianni, 2013). The average particle sizes of the optimized formulations were 174.46 ± 15.25 nm and 262.38 ± 11.85 nm for PLGA-PVP-NPs (F2) and PLGA-TPGS-NPs (F5), respectively (Table 1).

As for NPs polydispersity, which indicates the NPs size distributions, the lower the value, the more stable dispersion of the NPs in the medium. The developed formulations had polydispersity index values of 0.297 ± 0.015 for F2 and 0.255 ± 0.011 for F5. The zeta potential values of F2 and F5 were -15.82 ± 3.69 mV and 15.14 ± 2.81 mV, respectively (Table 1). These values favor the stability of the NPs dispersion because of electrostatic repulsion between the similar charges that would prevent the NPs aggregation. The positively charged PLGA-TPGS-NPs, however, offer an additional advantage by their ability to strongly adhere with the negatively charged mucin layer of precorneal and corneal surfaces, prolonging the residence time of the NPs. Collectively, these results emphasize the superiority of TPGS as a stabilizer compared to PVP as it was able to emulsify more ACY, yielding a smaller NP having a positive zeta potential, optimal for ocular drug delivery purposes.

3.2. Physicochemical characteristics of the ophthalmic preparation

In order to evaluate the suitability of the optimized PLGA-TPGS-NPs formulation for *in vivo* use, we evaluated its physicochemical parameters such as clarity, pH, refractive index, surface tension, and viscosity and compared it to that of acyclovir aqueous solution (ACY-AqS) (Table 2A). The pH values for ACY-AqS and PLGA-TPGS-NPs were 6.78 ± 0.27 and 6.88 ± 0.23, respectively. The obtained pH was tolerable for ophthalmic application and the values changed negligibly during the 30 days storage period. The acceptable pH range for ophthalmic preparations is 7.2 ± 0.2 (Lim et al., 2014; USP, 2016), however, any slight pH deviation can be buffered by tear fluids. The refractive index values for ACY-AqS and PLGA-TPGS-NPs were close to the refractive index of tear fluid and lachrymal fluid (1.34–1.36) (Craig et al., 1995). The surface tension measurements for ACY-AqS and PLGA-TPGS-NPs were

Table 2
Physicochemical parameters of the ACY-AqS and PLGA-TPGS-NPs determined at 25 °C (A); and corneal permeation parameters of ACY from the two formulations (B); (values were expressed in mean ± SD, n = 3).

(A) Physicochemical parameters			
Parameters	Time points	ACY-AqS	PLGA-TPGS-NPs
Clarity	Initially	Clear	Clear
	After 30 days	Clear	Clear
pH	Initially	6.78 ± 0.27	6.88 ± 0.23
	After 30 days	6.89 ± 0.25	7.21 ± 0.12
Refractive index	Initially	1.332 ± 0.009	1.353 ± 0.008
	After 30 days	1.345 ± 0.007	1.367 ± 0.003
Surface tension	Initially	39.53 ± 1.02	41.28 ± 1.04
($mN \cdot m^{-1}$)	After 30 days	42.27 ± 1.04	45.13 ± 1.03
Viscosity (mPa·s)	Initially	30.15 ± 1.07	35.42 ± 1.85
	After 30 days	33.27 ± 1.94	39.35 ± 2.05

(B) Corneal permeation parameters		
Parameters	PLGA-TPGS-NPs (0.28%, w/v of ACY)	ACY-AqS (0.28%, w/v of ACY)
Cumulative amount permeated ($\mu g\ cm^{-2}$ at 6 h)	1872.691 ± 42.582	1933.109 ± 12.895
pH	7.01 ± 0.09	7.24 ± 0.15
Steady-state flux, J ($\mu g\ cm^{-2}\ h^{-1}$)	521.541 ± 21.731	365.765 ± 13.861
Permeability coefficient, P (cm h^{-1})	$(18.627 \pm 0.0077) \times 10^{-2}$	$(13.063 \pm 0.0049) \times 10^{-2}$

39.53 ± 1.02 mN·m^{-1} and 41.28 ± 1.04 mN·m^{-1} respectively, which are marginally less than the normal range for lachrymal fluid (40–50 mN·m^{-1}) (Hotujac Grgurevic et al., 2017; Tiffany et al., 1989) (Table 2-A). Therefore, we assumed that the ACY-AqS and NPs dispersion would mix without any difficulty with precorneal film constituents and would retain satisfactory spreading effect on corneal and precorneal surfaces, which in turn extend the corneal and precorneal retention of the formulations and would improve the ACY ocular bioavailability.

The viscosity values for ACY-AqS and PLGA-NPs were 30.15 ± 1.07 mPa·s and 35.42 ± 1.85 mPa·s, respectively. The obtained values suggested relatively easy dispensing and filtration sterilization of the products. In addition, these values were slightly higher than that of the normal solution viscosity values (20 mPa·s) for ophthalmic preparations (Troy and Beringer, 2006), which prolongs corneal and precorneal retention of the formulations without blurring of vision.

3.3. In-vitro drug release and mechanism of release kinetics

The biodegradation of the polymer and the consequent drug release from NPs are of a prime importance in the development of polymeric NPs. Bulk or matrix erosion is considered the primary degradation pathway for PLGA, which take place due to the splitting of the ester bonds in the backbone of PLGA (Bala et al., 2004).

In this study, the *in-vitro* drug release profile from the two optimized NPs gave an initial burst release of ACY up-to 8 h followed by a controlled release of drug up-to 14 h then a slower exponential sustained release till 72 h. For PLGA-PVP-NPs and PLGA-TPGS-NPs, the cumulative amounts of drug released after 72 h were $64.67 \pm 4.29\%$ and $66.99 \pm 4.78\%$, respectively. The release of drug from NPs depends on factors like desorption of the surface adsorbed drug, diffusion of drug through the matrix of NPs, NPs matrix erosion and a combination of diffusion and erosion processes (surface and bulk or matrix). The plot of cumulative amount of drug released versus time for 72 h (Fig. 1) indicated the release of ACY was not influenced by the amount of PLGA used but depends on the type of stabilizer used in the two NPs. Generally,
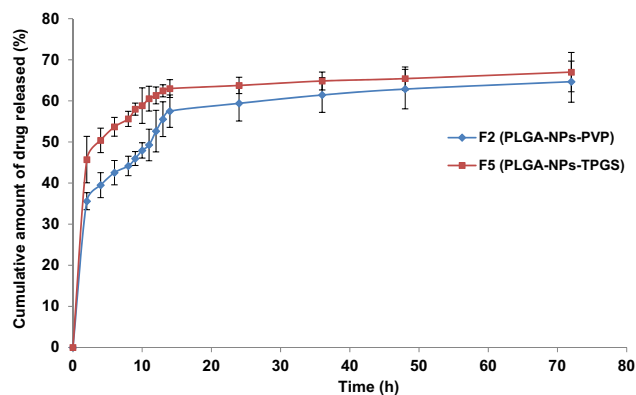
Fig. 1. *In vitro* drug release profiles of PLGA-NPs in simulated tear fluid (STF, pH 7.4), F5 representing more sustained release property than that of F2.

different release rates are attributed to different sizes of the NPs, but here the size of PLGA-PVP-NPs and PLGA-TPGS-NPs are almost comparable, hence size had no effect on the cumulative amount of ACY released in the two NPs. The initial rapid release of ACY could be as a result of the process by which PLGA undergoes biodegradation which exposes the drug closer to the surface (that could be free or loosely bound), in contact with the medium, to water that solubilizes the drug abruptly (Bhosale et al., 2011; Jain, 2000).

The release pattern of ACY from PLGA-PVP-NPs and PLGA-TPGS-NPs was fitted in release kinetic models to recognize the nature of curves obtained. The curve-fitting technique has shown the release pattern of ACY from PLGA-PVP-NPs and PLGA-TPGS-NPs followed the Korsmeyer-Peppas release kinetics model. This was supported by the relatively higher values of correlation coefficients (R^2) in the straight line equations obtained through Korsmeyer-Peppas release equation log $(M_0 - M_t) = \log k + n \log t$, as well as the obtained diffusion-exponent (n-values) as compared to the other sets of release models. The n-values are supportive to determine the release mechanism (when it falls between 0 and 0.5 the release mechanism is Fickian diffusion and 0.5–1.0, the mechanism is non-Fickian). The calculated n-values were found in the range of 0.0457–0.0799 (Table 3), proposing the release of ACY from PLGA-NPs was functioned through the Fick's law of diffusion.

3.4. Physical stability of ACY-PLGA-NPs dispersion

The physical stability at different temperatures was observed under light microscopy for the optimized formulations. No aggregation was observed when stored at 4 °C for 10 days, but few aggregates of NPs was seen after 10 days of storage at 25 °C. Upon increasing the temperature to 37 °C, PLGA-PVP-NPs were aggregated into larger particles that were not re-dispersed easily even after vortexing and sonication, which was not the case with PLGA-TPGS-NPs. Storing NPs at 50 °C for 10 days resulted in amal-

gamation of PLGA-PVP-NPs into a sticky, solid but elastic form, which was not the case in PLGA-TPGS-NPs. To confirm our findings, we employed SEM to take a closer look at the two systems. The PLGA-PVP-NPs were not aggregated at 4 °C (Fig. 2A) and 25 °C (Fig. 2B). At higher temperatures though, the PLGA-PVP-NPs arranged themselves to form a compact, fibrous, and complex network (Fig. 2C and D). In contrast, the PLGA-TPGS-NPs were readily re-dispersed and have shown the particles in segregated form (Fig. 3A–D). The formation of the complex network with PLGA-PVP-NPs might be due to the complete evaporation of residual solvent (acetone) at higher temperatures (37 °C and 50 °C) during storage or the melting of PVP (De and Robinson, 2004). Overall, SEM has shown that the magnitude of aggregation was higher in case of PVP based NPs as compared to TPGS based.

Investigating the stability of the developed NPs up to 3 months at 25 °C involved analyzing the particle-size, polydispersity index, zeta-potential, encapsulation, ACY loading, and cumulative release of ACY. After 1 week, little changes were observed in both optimized formulations (Table 4). An increase in the particle size, polydispersity, and absolute zeta-potential values as well as a decrease in encapsulation, drug loading and cumulative amount of drug released were observed in both formulations, after one and three months. We observed that the particle size changes in case of PLGA-PVP-NPs was overall higher compared to PLGA-TPGS-NPs, which was also indicated by the aggregation described earlier (Table 4). The stability results indicate that the amount of TPGS on the surface of nanoparticles is sufficiently high to prevent the colloidal destabilization by steric hindrance, hence showing little to no changes in polydispersity even after 3 months at 25 °C storage of PLGA-TPGS-NPs dispersion in STF. Therefore, instead of reversible flocculation, irreversible coagulation occurred for the PLGA-NPs, indicating that they exhibited the anticipated behavior for lyophobic colloidal systems (Santander-Ortega et al., 2007).

3.5. Corneal permeation study

It is proposed that the delivery of smaller sized NPs facilitate transcorneal and precorneal passage through inter- and intracellular junctions as a result of enhanced precorneal retention (Zhang and Feng, 2006). The corneal permeation area i.e. aperture of transdermal diffusion cell was 0.636 cm^2, volume of release medium in the receptor compartment was 6.9 mL and initial ACY concentrations was 2800 µg mL^{-1} in the receptor compartment. The amount of ACY permeated per unit area per unit time (permeation-flux, J) and permeation coefficients (P) were calculated for ACY-AqS and PLGA-TPGS-NPs (Table 2B).

The drainage of precorneal fluid is one of the main reasons for low ocular bioavailability of any drug (Agrahari et al., 2016; du Toit et al., 2011). A large fraction of instilled volume (approximately 80–90%) is drained into the nasolacrimal duct, nasolacrimal drainage helps to maintain the precorneal fluid volume of about 7–10 µL at any time (Agrahari et al., 2016; Djebli et al., 2017). There are certain factors those influence the nasolachrimal drainage rate,

Table 3
Release kinetics model analysis by fitting the *in-vitro* drug release data.[*]

Release models	Model equations	Release mechanism	PLGA-PVP-NPs (F2)		PLGA-TPGS-NPs (F5)	
			"R^2-value"	"n-value"	""R^2-value"	"n-value"
Zero order	$M_0 - M_t = kt$	Diffusion Mechanism	0.6611	–	0.5163	–
First order	$\ln M_t = \ln M_0 + kt$	Fick's first law, diffusion mechanism	0.7211	–	0.5749	–
Higuchi's matrix	$M_0 - M_t = kt^{1/2}$	Diffusion medium based mechanism in Fick's first law	0.8186	–	0.6964	–
Korsmeyer-Peppas	$\log (M_0 - M_t) = \log k + n \log t$	Semi empirical model, diffusion based mechanism	0.9167	0.07993	0.8661	0.04576
Hixson-Crowell	$M_0^{1/3} - M_t^{1/3} = k_s t$	Erosion release mechanism	0.7013	–	0.5551	–

[*] M_0 = "initial amount of drug, M_t = amount of drug remaining at time (t), k = rate constant, T_i = location parameter, α = scale parameter, m = accumulated fraction of the drug, β = shape factor and n = diffusion exponent".
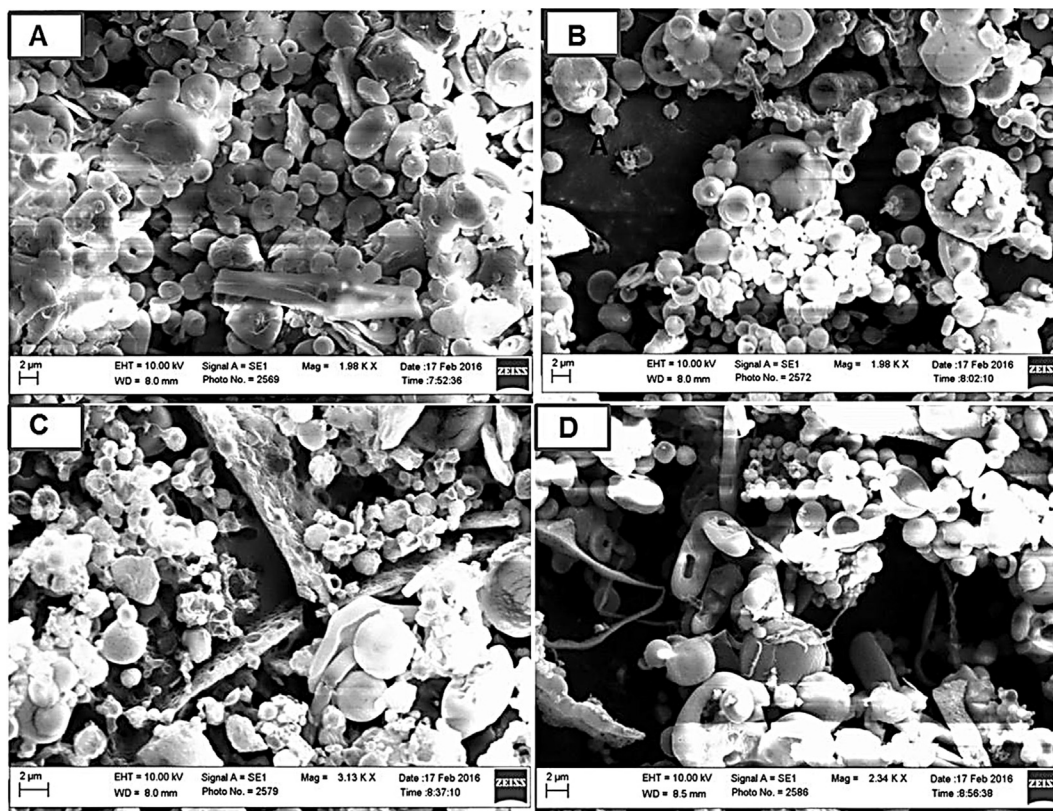
Fig. 2. Scanning electron micrographs (SEM) illustrating the effect of storage temperature on the aggregation behavior of PLGA-PVP-NPs (F2) storing at 4 °C, 25 °C, 37 °C, and 50 °C for 10 days.
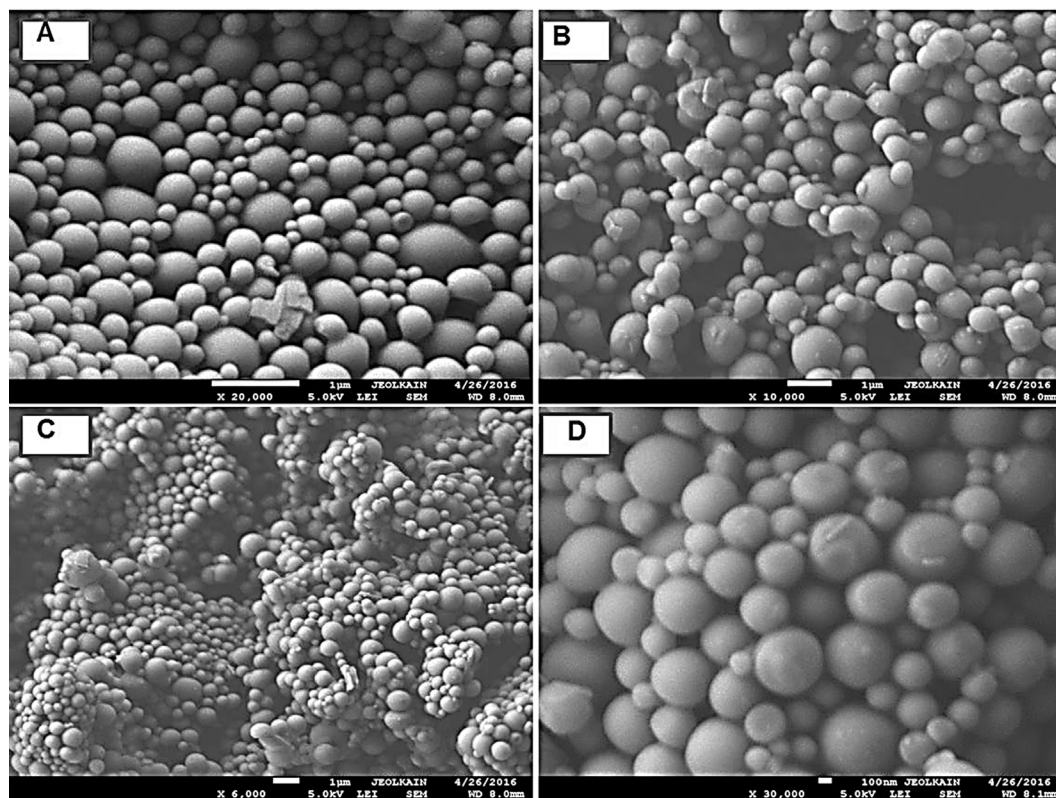

Fig. 3. Scanning electron micrograph (SEM) illustrating the effect of storage temperature on the aggregation behavior of PLGA-TPGS-NPs (F5) storing at 4 °C, 25 °C, 37 °C, and 50 °C for 10 days.

Table 4
Storage effect on particle-size, zeta-potential, polydispersity, encapsulation, loading and cumulative drug release of PLGA-NPs for 3 months at 25 °C (mean ± SD, n = 3).

At 3 months storage	Particle-size (nm)	Polydispersity index	Zeta-potential (mV)	Encapsulation (% EE)	ACY loading (% DL)	Cumulative release of ACY (%)
Initially						
PLGA-NPs-PVP (F2)	174.46 ± 15.25	0.297 ± 0.015	−15.82 ± 3.69	60.25 ± 4.92	6.75 ± 1.32	64.67 ± 4.29
PLGA-NPs-TPGS (F5)	262.38 ± 11.85	0.255 ± 0.011	+15.14 ± 2.81	74.12 ± 6.19	8.65 ± 1.09	66.99 ± 4.78
After 1 week						
PLGA-NPs-PVP (F2)	187.25 ± 9.25	0.302 ± 0.014	−16.25 ± 2.74	60.11 ± 2.75	6.25 ± 1.15	63.75 ± 2.34
PLGA-NPs-TPGS (F5)	271.15 ± 8.51	0.261 ± 0.017	+15.35 ± 1.98	73.75 ± 3.05	7.99 ± 1.24	66.38 ± 2.18
After 1 month						
PLGA-NPs-PVP (F2)	205.32 ± 11.37	0.312 ± 0.025	−15.23 ± 2.11	60.01 ± 1.87	6.19 ± 1.07	61.25 ± 1.75
PLGA-NPs-TPGS (F5)	302.25 ± 9.75	0.293 ± 0.031	+16.27 ± 2.43	61.26 ± 1.24	7.81 ± 1.14	65.58 ± 1.86
After 3 months						
PLGA-NPs-PVP (F2)	273.18 ± 12.43	0.345 ± 0.027	−17.26 ± 2.17	58.23 ± 1.19	6.03 ± 1.02	60.12 ± 1.25
PLGA-NPs-TPGS (F5)	354.63 ± 15.45	0.312 ± 0.008	+17.25 ± 2.08	60.34 ± 1.75	7.79 ± 1.05	63.78 ± 1.97

which are as; (i) instilled volume (higher the instilled volume higher the rate of solution drainage), therefore no extra volume of formulation can be administered during the ocular delivery, (ii) viscosity (high viscosity of the instilled dose extend the pre-corneal retention of the dosage form and hence improved drug absorption), (iii) pH (the physiological pH of tear fluid is 7.4, but the buffering capacity of tear fluid is very high so slightly variable pH of the ACY-PLGA-NPs were buffered by the tear fluid to the ocular physiological pH, (iv) tonicity and type of drug (ACY being a class-III drug having high solubility but low permeability (Parr et al., 2016; Wu and Benet, 2005) but PLGA-based ACY-NPs could easily penetrate through the corneal and conjunctival epithelial layer, moreover, mannitol was added in the formulation to make them isotonic with tear fluid) (Singh and Shrivastava, 2011). Thus, by managing the above factors nasolachrimal drainage could be maintained throughout the experiment.

The sodium salt of acyclovir was used to prepare the PLGA-NPs and ACY-AqS for ocular use. ACY is slightly soluble in water at 25 °C having a solubility of 1.2–1.6 mg/mL, depending on the pH of the medium. ACY is an ampholyte with both the weak acid and basic groups with the reported pK_a values of 2.16 and 9.04 at 37 °C (Kasim et al., 2004). The reported partition-coefficient (log P) value of ACY in n-octanol at 25 °C is −1.59. Normally, the molecules with permeability range 70% to 100% absorbed have P_{app} values greater than 10×10^{-6} cm s^{-1}. However, ACY permeability coefficient ranged 0.12–2.0 × 10^{-6} cm s^{-1}, indicating the low permeability of ACY (Bergstrom et al., 2003). Thus, it could be hypothesized that as the pH of ACY-AqS and suspension of PLGA-NPs shifted toward the pH of tears, a large fraction of ACY would become in the unionized form, which promotes transcorneal passage of ACY. The permeation of ACY from its aqueous solution was high initially as large fraction of ACY was unionized at pH 6.78 ± 0.27, so increasing the efficient permeation while buffering the formulations (Cohen et al., 2012). From the values of permeation parameters (Table 2B), it was concluded that PLGA-TPGS-NPs facilitated sustained release of ACY as compared to ACY-AqS. Another factor that could contribute to the sustained release and high permeation of ACY from PLGA-TPGS-NPs is the presence of TPGS, which might have inhibited the P-glycoprotein resulting in enhanced ACY transcorneal permeation (Dintaman and Silverman, 1999).

3.6. Ocular irritation study

The acute and long-term ocular irritation potential of ACY loaded PLGA-TPGS-NPs was performed in rabbit eyes with normal saline as control. After frequent instillations of PLGA-NPs dispersion, a slight irritation was observed in one treated animal (Fig. 4 and Supplementary Table 1). Fig. 4A, represents the normal condition of untreated eye. The treated right eyes of animals showed mild redness in the conjunctival area (Fig. 4B) at the first hour post administration. The redness increased further at the third hour (Fig. 4C). The redness and inflammation in the conjunctival area were reduced at sixth hour (Fig. 4D), and the redness and inflammation completely disappeared at the twelfth hour (Fig. 4E). We should point out that in one animal some mucoidal discharge (grade 1) was observed while there was no discharge in the remaining animals. None of the animals showed any sign of tissue damage to the conjunctiva. The results of the irritation studies suggested the relative safety of ACY loaded PLGA-TPGS-NPs as the nanocarrier system was non-toxic and non-irritant to the eyes, paving the way for its *in vivo* use.

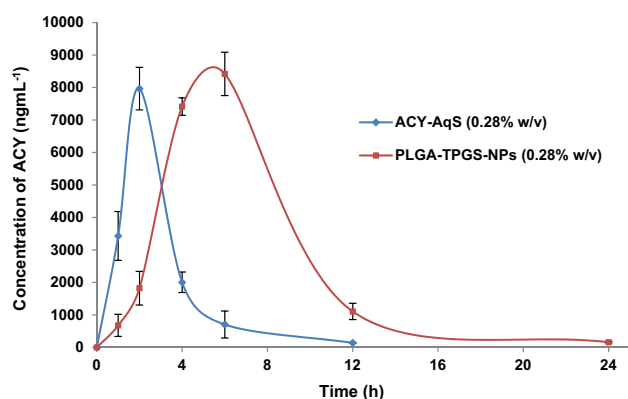### 3.7. Detection of ACY in aqueous humor

The validated UPLC-UV method was successfully applied for ACY quantification in aqueous humor of rabbits' eyes after topical administration of ACY-AqS and PLGA-TPGS-NPs (Supplementary material). The detected concentrations of ACY in aqueous humor samples extracted from rabbit eyes at 1, 2, 4, 6, 12 and 24 h are demonstrated in Fig. 5. In ACY-AqS treated rabbits, ACY concentration in aqueous humor was noticed up to 6th h of experiment, after that ACY was undetected, which might be due to rapid corneal and precorneal loss of ACY in its solution form. However, in PLGA-TPGS-NPs treated animals, ACY was detected in adequate amount in aqueous humors up to 24th h of the experiment.

The rate and extent of absorption and permeation of ACY from PLGA-TPGS-NPs and reference ACY-AqS were analyzed by comparing the pharmacokinetic parameters like, C_{max}, T_{max}, $t_{1/2}$, AUC and MRT for both the treatment groups (Table 5). The pharmacokinetic parameters were calculated by using PK-Solver software. The aqueous humor ACY concentration-time plot was smooth enough and found appropriate to accomplish the ocular pharmacokinetic data analysis of the formulations. By comparing the obtained pharmacokinetic data for the two formulations it was found that PLGA-NPs has shown significantly ($p < 0.05$) higher ocular bioavailability of ACY than that of ACY-AqS. The noticeable, 2.78- and 2.76-times higher AUC$_{0-24h}$ and AUC$_{0-inf}$ were observed, respectively with the PLGA-TPGS-NPs as compared to ACY-AqS. The $t_{1/2}$ of ACY from NPs was significantly high than that of ACY-AqS with 1.71-times increased value. A significant (2.20-fold) increase in mean residence time was calculated for PLGA-TPGS-NPs as compared to ACY-AqS.

The elevated values of pharmacokinetic parameters in case of NPs treated animals indicating the prolonged precorneal retention of PLGA-TPGS-NPs might be attributed to the following reasons.
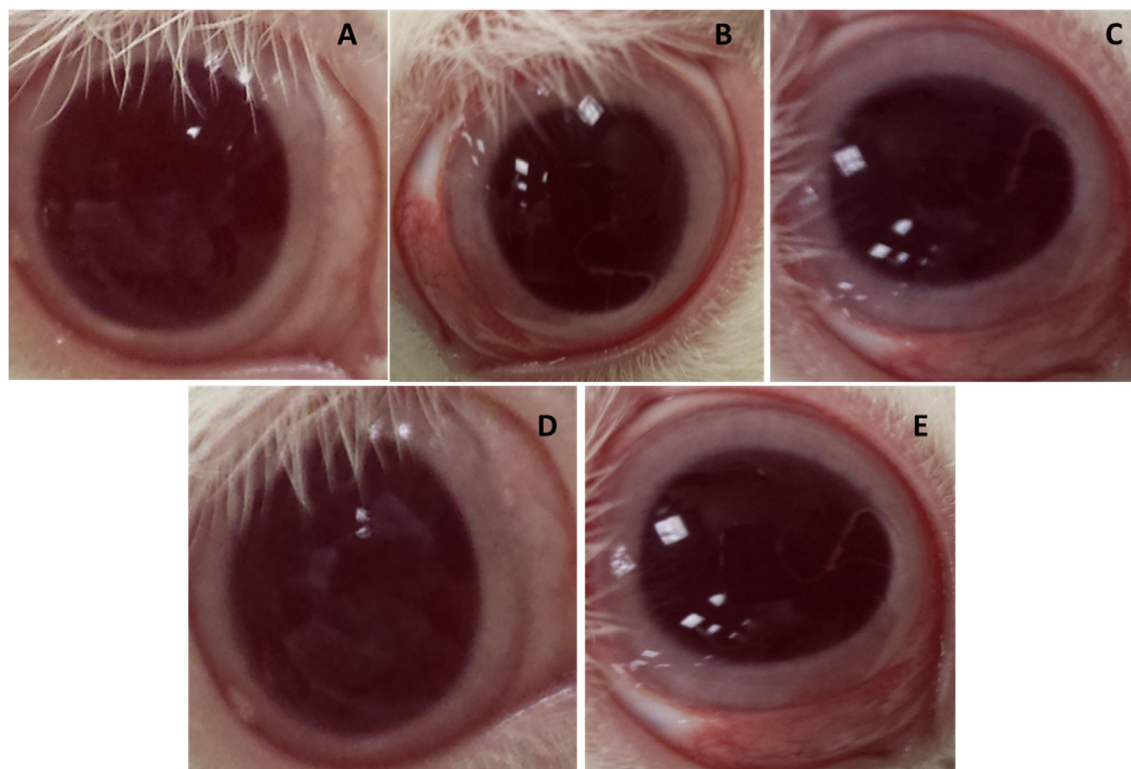
Fig. 4. The redness and inflammation in rabbit eyes due to instillation of PLGA-TPGS-NPs (F5) dispersion at different time intervals. Normal eye (A), mild redness and inflammation at 1st h (B), intense redness and mild inflammation at 3rd h (C), reduced redness and inflammation at 6th h (D), complete disappearance of redness and inflammation at 12th h (E).

Fig. 5. Acyclovir concentrations in aqueous humor following topical ocular instillation of F5 and ACY-AqS in rabbit eyes (mean ± SD, $n = 3$).

Table 5
Pharmacokinetic parameters of ACY in aqueous humor after topical administration of ACY-AqS and PLGA-TPGS-NPs (mean ± SD, $n = 3$).

Parameters	Values for ACY-AqS	Values for PLGA-TPGS-NPs (F5)
$t_{1/2}$ (h)	1.908 ± 0.173	3.264 ± 0.067
T_{max} (h)	2.0 ± 0.0	6.0 ± 0.0
C_{max} (ng mL^{-1})	7965.024 ± 312.359	8419.081 ± 668.077
AUC_{0-t} (ng mL^{-1}·h)	22627.241 ± 839.556	62816.113 ± 4596.857
AUC_{0-inf} (ng mL^{-1}·h)	23013.076 ± 822.584	63546.783 ± 4727.427
$AUC_{0-t/0-inf}$	0.9832 ± 0.007	0.9882 ± 0.0013
$AUMC_{0-inf}$ (ngmL^{-1}·h^2)	71012.729 ± 12115.95	431247.299 ± 50560.543
MRT_{0-inf} (h)	3.072 ± 0.219	6.771 ± 0.291

First, the positive zeta potential of PLGA-TPGS-NPs induced electrostatic attraction with the negatively charged mucin layer of cornea and conjunctiva of rabbits' eye. This electrostatic interaction might have enhanced the ocular retention of PLGA-TPGS-NPs resulting in high transcorneal permeation of ACY as compared to ACY-AqS. The high aqueous-miscibility and structure-property relationship of vitamin E-TPGS suggested that it may exceptionally meet the requirement for increased ACY solubility through micellar solubilization, so increased permeability and prevented crystallization of ACY which in turn enhanced its ocular bioavailability. The TPGS helps in paracellular diffusion of ACY as a modulator of tight cellular junctions; TPGS is also involved in transcellular diffusion modified by an apically polarized efflux mechanism as it inhibits the efflux system and enhances the permeability of the drug. Overall, TPGS exerts a protective effect on corneal membrane layer membrane against free-radical damage and enhanced the absorption flux of ACY across corneal barrier by increasing its solubility and permeability (Yu et al., 1999). TPGS being a nonionic surfactant, modulates P-glycoprotein efflux transport via P-glycoprotein-ATPase inhibition (Collnot et al., 2010) and causing the improved ocular bioavailability of acyclovir via PLGA-TPGS-NPs. The pharmacokinetic parameters obtained by the PLGA-TPGS-NPs suggesting the potential of the developed nanocarrier for the topical ocular ACY delivery in treating ocular infections such as herpes simplex virus epithelial keratitis and varicella zoster virus caused herpes zoster ophthalmicus.

4. Conclusions

The optimized PLGA-TPGS-NPs we developed where deemed suitable for ocular drug delivery. While the effectiveness of the PLGA-TPGS-NPs against ocular viral infections is yet to be confirmed, the developed nanosystem has shown promise in its ability

to deliver the ACY safely and efficiently to the eye. Future work will capitalize on the many advantages of the developed nanocarrier to further enhance its properties as an optimal ocular drug delivery system.

Acknowledgement

Appendix A. Supplementary material

Supplementary data to this article can be found online at https://doi.org/10.1016/j.jsps.2018.11.011.

References

Agrahari, V., Mandal, A., Trinh, H.M., Joseph, M., Ray, A., Hadji, H., Mitra, R., Pal, D., Mitra, A.K., 2016. A comprehensive insight on ocular pharmacokinetics. Drug Deliv. Transl. Res. 6, 735–754.

Akhter, S., Ramazani, F., Ahmad, M.Z., Ahmad, F.J., Rahman, Z., Bhatnagar, A., Storm, G., 2013. Ocular pharmacoscintigraphic and aqueous humoral drug availability of ganciclovir-loaded mucoadhesive nanoparticles in rabbits. Eur. J. Nanomed. 5, 159–167.

Alshamsan, A., 2014. Nanoprecipitation is more efficient than emulsion solvent evaporation method to encapsulate cucurbitacin I in PLGA nanoparticles. Saudi Pharmaceut. J. 22, 219–222.

Attama, A.A., Reichl, S., Muller-Goymann, C.C., 2008. Diclofenac sodium delivery to the eye: in vitro evaluation of novel solid lipid nanoparticle formulation using human cornea construct. Int. J. Pharm. 355, 307–313.

Bala, I., Hariharan, S., Kumar, M.N., 2004. PLGA nanoparticles in drug delivery: the state of the art. Crit. Rev. Ther. Drug Carrier Syst. 21, 387–422.

Bergstrom, C.A., Strafford, M., Lazorova, L., Avdeef, A., Luthman, K., Artursson, P., 2003. Absorption classification of oral drugs based on molecular surface properties. J. Med. Chem. 46, 558–570.

Bhosale, U., Kusum, D.V., Jain, N., 2011. Formulation and optimization of mucoadhesive nanodrug delivery system of acyclovir. J. Young Pharm. 3, 275–283.

Chen, H., Zheng, Y., Tian, G., Tian, Y., Zeng, X., Liu, G., Liu, K., Li, L., Li, Z., Mei, L., Huang, L., 2011. Oral delivery of DMAB-modified docetaxel-loaded PLGA-TPGS nanoparticles for cancer chemotherapy. Nanoscale Res. Lett. 6, 4.

Cholkar, K., Patel, S.P., Vadlapudi, A.D., Mitra, A.K., 2013. Novel strategies for anterior segment ocular drug delivery. J. Ocul. Pharmacol. Ther. 29, 106–123.

Cohen, A.E., Assang, C., Patane, M.A., From, S., Korenfeld, M., 2012. Evaluation of dexamethasone phosphate delivered by ocular iontophoresis for treating noninfectious anterior uveitis. Ophthalmology 119, 66–73.

Collnot, E.M., Baldes, C., Schaefer, U.F., Edgar, K.J., Wempe, M.F., Lehr, C.M., 2010. Vitamin E TPGS P-glycoprotein inhibition mechanism: influence on conformational flexibility, intracellular ATP levels, and role of time and site of access. Mol. Pharm. 7, 642–651.

Craig, J.P., Simmons, P.A., Patel, S., Tomlinson, A., 1995. Refractive index and osmolality of human tears. Optom. Vis. Sci. 72, 718–724.

Danhier, F., Ansorena, E., Silva, J.M., Coco, R., Le Breton, A., Preat, V., 2012. PLGA-based nanoparticles: an overview of biomedical applications. J. Control. Release 161, 505–522.

De, S., Robinson, D.H., 2004. Particle size and temperature effect on the physical stability of PLGA nanospheres and microspheres containing Bodipy. AAPS PharmSciTech 5, e53.

Diebold, Y., Jarrin, M., Saez, V., Carvalho, E.L., Orea, M., Calonge, M., Seijo, B., Alonso, M.J., 2007. Ocular drug delivery by liposome-chitosan nanoparticle complexes (LCS-NP). Biomaterials 28, 1553–1564.

Dintaman, J.M., Silverman, J.A., 1999. Inhibition of P-glycoprotein by D-alpha-tocopheryl polyethylene glycol 1000 succinate (TPGS). Pharm. Res. 16, 1550–1556.

Djebli, N., Khier, S., Griguer, F., Coutant, A.L., Tavernier, A., Fabre, G., Leriche, C., Fabre, D., 2017. Ocular drug distribution after topical administration: population pharmacokinetic model in rabbits. Eur. J. Drug Metab. Pharmacokinet. 42, 59–68.

Draize, J.H., Woodard, G., Calvery, H.O., 1944. Methods for the study of irritation and toxicity of substances applied topically to the skin and mucous membranes. J. Pharmacol. Exp. Ther. 82, 377–390.

du Toit, L.C., Pillay, V., Choonara, Y.E., Govender, T., Carmichael, T., 2011. Ocular drug delivery – a look towards nanobioadhesives. Expert Opin. Drug Deliv. 8, 71–94.

Fabiano, A., Chetoni, P., Zambito, Y., 2015. Mucoadhesive nano-sized supramolecular assemblies for improved pre-corneal drug residence time. Drug Dev. Ind. Pharm. 41, 2069–2076.

Fangueiro, J.F., Andreani, T., Fernandes, L., Garcia, M.L., Egea, M.A., Silva, A.M., Souto, E.B., 2014. Physicochemical characterization of epigallocatechin gallate lipid nanoparticles (EGCG-LNs) for ocular instillation. Colloids Surf. B Biointerfaces 123, 452–460.

Grenha, A., Seijo, B., Serra, C., Remunan-Lopez, C., 2007. Chitosan nanoparticle-loaded mannitol microspheres: structure and surface characterization. Biomacromolecules 8, 2072–2079.

Hotujac Grgurevic, M., Juretic, M., Hafner, A., Lovric, J., Pepic, I., 2017. Tear fluid-eye drops compatibility assessment using surface tension. Drug Dev. Ind. Pharm. 43, 275–282.

Jain, R.A., 2000. The manufacturing techniques of various drug loaded biodegradable poly(lactide-co-glycolide) (PLGA) devices. Biomaterials 21, 2475–2490.

Kalam, M.A., 2016a. Development of chitosan nanoparticles coated with hyaluronic acid for topical ocular delivery of dexamethasone. Int. J. Biol. Macromol. 89, 127–136.

Kalam, M.A., 2016b. The potential application of hyaluronic acid coated chitosan nanoparticles in ocular delivery of dexamethasone. Int. J. Biol. Macromol. 89, 559–568.

Kasim, N.A., Whitehouse, M., Ramachandran, C., Bermejo, M., Lennernas, H., Hussain, A.S., Junginger, H.E., Stavchansky, S.A., Midha, K.K., Shah, V.P., Amidon, G.L., 2004. Molecular properties of WHO essential drugs and provisional biopharmaceutical classification. Mol. Pharm. 1, 85–96.

Law, S.L., Huang, K.J., Chiang, C.H., 2000. Acyclovir-containing liposomes for potential ocular delivery. Corneal penetration and absorption. J. Control. Release 63, 135–140.

Lim, L.T., Ah-Kee, E.Y., Collins, C.E., 2014. Common eye drops and their implications for pH measurements in the management of chemical eye injuries. Int. J. Ophthalmol. 7, 1067–1068.

Ma, Y., Zheng, Y., Liu, K., Tian, G., Tian, Y., Xu, L., Yan, F., Huang, L., Mei, L., 2010. Nanoparticles of poly(lactide-co-glycolide)-d-a-tocopheryl polyethylene glycol 1000 succinate random copolymer for cancer treatment. Nanoscale Res. Lett. 5, 1161–1169.

McCall, R.L., Sirianni, R.W., 2013. PLGA nanoparticles formed by single- or double-emulsion with vitamin E-TPGS. J Vis Exp, 51015.

Naderkhani, E., Erber, A., Skalko-Basnet, N., Flaten, G.E., 2014. Improved permeability of acyclovir: optimization of mucoadhesive liposomes using the phospholipid vesicle-based permeation assay. J. Pharm. Sci. 103, 661–668.

Nagarwal, R.C., Kant, S., Singh, P.N., Maiti, P., Pandit, J.K., 2009. Polymeric nanoparticulate system: a potential approach for ocular drug delivery. J. Control. Release 136, 2–13.

Parr, A., Hidalgo, I.J., Bode, C., Brown, W., Yazdanian, M., Gonzalez, M.A., Sagawa, K., Miller, K., Jiang, W., Stippler, E.S., 2016. The effect of excipients on the permeability of BCS Class III compounds and implications for biowaivers. Pharm. Res. 33, 167–176.

Salama, A.H., Mahmoud, A.A., Kamel, R., 2015. A novel method for preparing surface-modified fluocinolone acetonide loaded PLGA nanoparticles for ocular use vitro and in vivo evaluations. AAPS PharmSciTech 17, 1159–1172.

Santander-Ortega, M.J., Csaba, N., Alonso, M.J., Ortega-Vinuesa, J.L., Bastos-Gonzalez, D., 2007. Stability and physicochemical characteristics of PLGA, PLGA: poloxamer and PLGA:poloxamine blend nanoparticles: a comparative study. Colloids Surf., A 296, 132–140.

Seyfoddin, A., Shaw, J., Al-Kassas, R., 2010. Solid lipid nanoparticles for ocular drug delivery. Drug Deliv. 17, 467–489.

Shen, J., Durairaj, C., Lin, T., Liu, Y., Burke, J., 2014. Ocular pharmacokinetics of intravitreally administered brimonidine and dexamethasone in animal models with and without blood-retinal barrier breakdown. Invest. Ophthalmol. Vis. Sci. 55, 1056–1066.

Silva, G.R., Caldeira, A.S., Damico, F.M., Takahashi, B.S., Silva-Cunha, A., Fialho, S.L., 2013. Analysis of acyclovir in vitreous humor by a validated HPLC method. Pharmazie 68, 235–239.

Singh, K., Shrivastava, A., 2011. Medical management of glaucoma: principles and practice. Indian J. Ophthalmol. 59 (Suppl), S88–92.

Stulzer, H.K., Tagliari, M.P., Murakami, F.S., Silva, M.A., Laranjeira, M.C., 2008. Development and validation of an RP-HPLC method to quantitate acyclovir in cross-linked chitosan microspheres produced by spray drying. J. Chromatogr. Sci. 46, 496–500.

Tiffany, J.M., Winter, N., Bliss, G., 1989. Tear film stability and tear surface tension. Curr. Eye Res. 8, 507–515.

Troy, D.B., Beringer, P., 2006. Remington: The Science and Practice of Pharmacy. Lippincott Williams & Wilkins, USA, p. 862.

USP, 2016. United States Pharmacopoeia 39-National Formulary 34th ed. U.S.P. Convention. Stationery Office, USA.

Warsi, M.H., Anwar, M., Garg, V., Jain, G.K., Talegaonkar, S., Ahmad, F.J., Khar, R.K., 2014. Dorzolamide-loaded PLGA/vitamin E TPGS nanoparticles for glaucoma therapy: pharmacoscintigraphy study and evaluation of extended ocular hypotensive effect in rabbits. Colloids Surf., B 122, 423–431.

Wu, C.Y., Benet, L.Z., 2005. Predicting drug disposition via application of BCS: transport/absorption/elimination interplay and development of a biopharmaceutics drug disposition classification system. Pharm. Res. 22, 11–23.

Yu, L., Bridgers, A., Polli, J., Vickers, A., Long, S., Roy, A., Winnike, R., Coffin, M., 1999. Vitamin E-TPGS increases absorption flux of an HIV protease inhibitor by enhancing its solubility and permeability. Pharm. Res. 16, 1812–1817.

Zhang, Y., Huo, M., Zhou, J., Xie, S., 2010. PKSolver: An add-in program for pharmacokinetic and pharmacodynamic data analysis in Microsoft Excel. Comput. Methods Programs Biomed. 99, 306–314.

Zhang, Z., Feng, S.S., 2006. The drug encapsulation efficiency, in vitro drug release, cellular uptake and cytotoxicity of paclitaxel-loaded poly(lactide)-tocopheryl polyethylene glycol succinate nanoparticles. Biomaterials 27, 4025–4033.

Zhang, Z., Lee, S.H., Gan, C.W., Feng, S.-S., 2008. In vitro and in vivo investigation on PLA-TPGS nanoparticles for controlled and sustained small molecule chemotherapy. Pharmaceut. Res. 25, 1925–1935. https://doi.org/10.1007/s11095-008-9611-6.

Zimmer, A., Kreuter, J.R., 1995. Microspheres and nanoparticles used in ocular delivery systems. Adv. Drug Deliv. Rev. Ocular Drug Deliv. 16, 61–73.